



Department of Management and Engineering
University of Padova



Tecnologie per il Calcolo Numerico
:: Centro Superiore di Formazione

TCN consortium

Sixth International Seminar on
**EXPERIMENTAL TECHNIQUES AND DESIGN
IN COMPOSITE MATERIALS**

Vicenza - ITALY 18-20th June 2003

**Department of Management and Engineering - University of Padova
Stradella S.Nicola 3 - 36100 VICENZA - ITALY**

PROCEEDINGS

Under the patronage of



REGIONE DEL VENETO

The Seminar

The application of composite materials in structural industrial components of large volume production is strongly growing year by year due to both increase in the demand and continuous improvements in the manufacturing processes associated to the reduction of the production cost. This highlights the need of reliable tools for an effective and safe design of composite components. For the complete and proper exploitation of composite materials further efforts are therefore required and the seminar aims to give a contribution in this direction, representing first of all a forum for researchers, scientist, engineers and designers, both of academic and industrial field, for exchanging ideas, proposing new solutions or even to put on the table questions still open. The development of design procedures, the integration between testing, design and process are therefore among the subjects expected to be discussed during the seminar.

The seminar main topics are:

- Mechanics of materials and mechanical properties
- NDT methods
- Damage characterization and analysis
- Fatigue and fracture
- Failure analysis
- Structural component design and optimization
- Processing and properties
- Analytical and numerical modeling

Scientific Committee

B. Atzori	University of Padova, I
F. Aymerich	University of Cagliari, I
P. W. R. Beaumont	University of Cambridge, UK
F. Bonollo	University of Padova, I
G. Caprino	University of Naples, I
T.W. Chou	University of Delaware, USA
T.W.Clyne	University of Cambridge, UK
I. Crivelli Viscont	University of Naples, I
M. S. Found	University of Sheffield, UK
A.Kelly	University of Cambridge, UK
P.Lazzarin	University of Padova, I
A. Mortensen	EPFL - Lausanne, CH
P. Priolo	University of Cagliari, I
M. Quaresimin	University of Padova, I
K. Schulte	TU Hamburg-Harburg, D
R. Talreja	Texas A&M University, USA
A. Tiziani	University of Padova, I

Seminar venue

The Seminar will take place at the Department of Management and Engineering - University of Padova - Stradella S.Nicola 3 - 36100 VICENZA - ITALY.

Web site

<http://www.gest.unipd.it/etdcm6/>

DELAMINATION GROWTH IN COMPOSITE PLATES UNDER COMPRESSIVE FATIGUE LOADS

S. BENNATI ^(*),^a and P. S. VALVO^a

^a Department of Structural Engineering, University of Pisa, Via Diotisalvi 2, I-56126 Pisa, Italy

ABSTRACT

A composite laminate containing a delamination is modelled as the union of two sublaminates partly bonded together by an elastic interface, in turn, represented by a continuous array of linear elastic springs acting in directions normal and tangential to the interface plane. A simple mechanical model, already presented by the authors in previous works, allows for determining the explicit expressions for the normal and tangential interlaminar stresses exerted between the sublaminates at the delamination front, as well as their peak values. It thus enables evaluating the individual contributions of modes I and II to the potential energy release rate G , as well as the value of the so-called mode-mixity angle. Based on the results obtained, a mode-dependent fatigue growth law can then be applied to take into account the simultaneous actions of the two different crack propagation modes. Thus, for any load level, predictions can be made on the number of cycles needed for a delamination to extend to a given length.

KEYWORDS: B. Fatigue, Interfacial strength; C. Buckling, Damage mechanics, Delamination.

INTRODUCTION

Delamination can arise in fibre-reinforced composite laminates as the result of many common events, such as manufacturing errors or low-velocity impacts [1, 2, 3]. When a laminated plate containing a delamination is loaded under compression, instability phenomena may promote further crack growth and, in some cases, lead to failure [4, 5, 6]. In order to model the process, the loss of

^(*) Corresponding author. Tel.: +39-050-835711; fax: +39-050-554597; e-mail: s.bennati@ing.unipi.it

stability can be studied through the methods of non-linear structural analysis, while delamination growth can be described through typical fracture mechanics.

Previous works by the authors [10, 11, 12] introduced a mechanical model for a delaminated plate subjected to monotonic compression. The plate is modelled as the union of two sublaminates, partly bonded together by an elastic interface, which is in turn represented by a continuous array of linear elastic springs acting in directions normal and tangential to the interface plane [see also 13, 14, 15, 16]. The model allows for determining the explicit expressions for the normal and tangential interlaminar stresses exerted between the sublaminates at the delamination front, as well as their peak values. It thus furnishes the individual contributions of modes I and II to the energy release rate G , as well as the so-called mode-mixity angle. Then, a mixed-mode growth criterion can be applied in order to predict the phenomena of delamination buckling and growth under static compressive loads.

The present paper extends the model outlined in the foregoing to include the case of delamination growth under cyclic compressive loads. In such cases, as the delaminated plate undergoes repeated buckling and unloading, damage progressively accumulates at the delamination front. As a consequence, an existing delamination may grow, even if the static growth criterion is not satisfied (i.e., if the energy release rate is less than the critical value). In what follows, a fatigue growth law, based on a mode-dependent critical energy release rate, is applied [17]. This enables predicting the number of cycles needed for a delamination to grow to a given length. The results may prove to be particularly useful, especially they have been obtained through explicit solutions, in shedding some light on the mechanisms underlying some very insidious failures and explaining a number of experimentally observed phenomena of delamination growth and arrest.

THE ELASTIC INTERFACE MODEL

Let us consider a rectangular laminated plate of length $2L$, width B , and thickness H , affected by a central, through-the-width delamination of length $2a$. The laminate is subjected to two compressive

loads of intensity P acting in the axial direction. The material is assumed to be homogeneous and linearly elastic, with orthotropy axes aligned with those of the global reference system $OXYZ$.

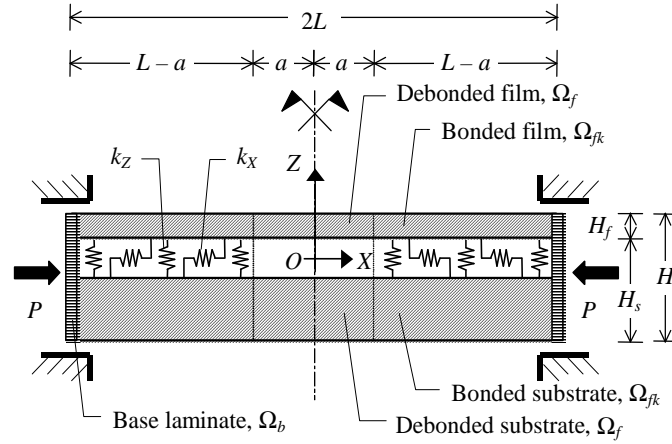


Fig. 1: The elastic interface model

The elastic interface model (Fig. 1) conceives of the delaminated plate as the union of two sublaminates, partly bonded by a continuous array of linear elastic springs. The two individual sublaminates are referred to as the ‘film’, which is the layer between the delamination plane and the nearest external surface (thickness H_f), and the ‘substrate’ (thickness $H_s = H - H_f$). The interface springs act in both the normal and tangential directions to the interface plane, where they are characterized by the elastic constants, k_z and k_x , respectively. The width B is assumed to be ‘very large’, so the sublaminates can be modelled as beam-plates. Hence, the ‘reduced’ Young modulus $E_X^* = E_X / (1 - \nu_{XZ} \nu_{ZX})$ is introduced, and all calculations refer to a unit width. According to the classical laminated plate theory, $A_f = E_X^* H_f$ and $D_f = E_X^* H_f^3 / 12$ are the extensional and bending stiffness of the film, respectively; $A_s = E_X^* H_s$ and $D_s = E_X^* H_s^3 / 12$ are those of the substrate, and $A = E_X^* H$ and $D = E_X^* H^3 / 12$ are those of the base laminate.

Under these assumptions, the differential equations of the equilibrium problem according to von Kármán’s plate theory have been derived and solved completely in closed form. The explicit expressions for the solution in the pre- and post-buckling phases are reported in the above-cited works [10, 11, 12]. Herein, we limit ourselves to recalling the fundamental results.

The pre-buckling phase is characterized by a linear relationship between the applied load, P , and the end displacement of the plate, u . During this phase, the sublaminates undergo uniform shortening, and the axial force is distributed between them in proportion to their extensional stiffness. This behaviour ceases when the axial force in the debonded film, Ω_f , equals the buckling load of the sublaminate. This is determined by numerically solving a non-linear transcendental equation, which yields the buckling load of the delaminated plate, P_B , i.e., the load applied to the base laminate at the incipient buckling of the film.

During the post-buckling phase, the substrate experiences axial shortening alone, while the film undergoes bending as well as shortening. Because of the different displacements of the two laminates, non-zero stresses arise in the interface springs. Moreover, the energy release rate, $G = -\partial\Pi/\partial a$ (Π is the total potential energy of the system), which is zero throughout the pre-buckling phase, starts to increase.

G is the sum of the contributions of mode I and II:

$$G = G_I + G_{II} \quad (1)$$

which are:

$$G_I = \frac{k_Z a_{fk}^2}{2} \frac{8\lambda}{\frac{2a}{\lambda} - \sin\left(\frac{2a}{\lambda}\right)} \left(a + \omega \tanh \frac{L-a}{\omega} \right) \frac{P - P_B}{A_s} \quad (2a)$$

$$G_{II} = \frac{k_X}{2} \left(\omega \tanh \frac{L-a}{\omega} \frac{P - P_B}{A_s} \right)^2 \quad (2b)$$

where $\lambda^2 = (A D_f) / (A_f P_B)$; $\omega^2 = [k_X (A_f^{-1} + A_s^{-1})]^{-1}$; and a_{fk} is a dimensionless integration constant.

Finally, the mode-mixity angle,

$$\psi = \arctan \sqrt{\frac{k_X G_{II}}{k_Z G_I}} \quad (3)$$

is deduced. By convention, this provides a measure of the relative amount of fracture modes through values ranging from 0° (pure mode I) to 90° (pure mode II).

STATIC DELAMINATION GROWTH

According to Griffith's classical criterion, crack growth is to be expected when G equals a critical value, G_C . In the original and simplest formulation, G_C is a material constant, measuring the so-called 'toughness'. Nevertheless, for anisotropic materials such as composite laminates, experimental determinations of G_C are markedly dependent on the propagation mode acting in the test performed (I or opening, II or sliding, III or tearing). Actually, the critical value measured in pure mode III tests, $G_{III C}$, is usually greater than that obtained in pure mode II tests, $G_{II C}$, which may, in turn, be much greater than the value measured in pure mode I tests, $G_{I C}$.

Under mixed-mode conditions, as all propagation modes are simultaneously active, the toughness equals an intermediate value. Thus, in order to predict crack growth, a mixed-mode criterion is to be adopted, by which G_C is considered to be a function of the relative amount of the different propagation modes. In particular, for plane problems, the critical energy release rate,

$$G_C(\psi) = \frac{G_{I C}}{1 + (\gamma - 1)\sin^2(\psi)} \quad (4)$$

where $\gamma = G_{I C} / G_{II C}$, may be conveniently defined as a function of the mode-mixity angle [9].

For the present model the energy release rate, G , in the post-buckling phase is an increasing function of the applied load, P , as shown by equations (1) and (2). Moreover, the mode-mixity angle, ψ , increases as either the load or the delamination length grows. For any assigned delamination length, it is possible to determine the load, $P_G(a)$, at which $G = G_C(\psi)$, and static delamination growth is expected. Fig. 2 shows the buckling load of the delaminated plate, P_B , and the static delamination growth load, P_G , as functions of the delamination half-length, a . The following numerical values have been adopted: $L = 100$ mm, $H = 10$ mm and $H_f = 1$ mm; $E_X = 54$ GPa and $\nu_{XZ} = 0.25$; $k_X = 17284$ N/mm³ and $k_Z = 23333$ N/mm³; $G_{I C} = 100$ J/m² and $G_{II C} = 1000$

J/m². The loads have been divided by the Euler load, $P_{\text{eul}} = \pi^2 D / L^2 = 4535.8 \text{ N/mm}$, and the delamination half-length has been divided by L .

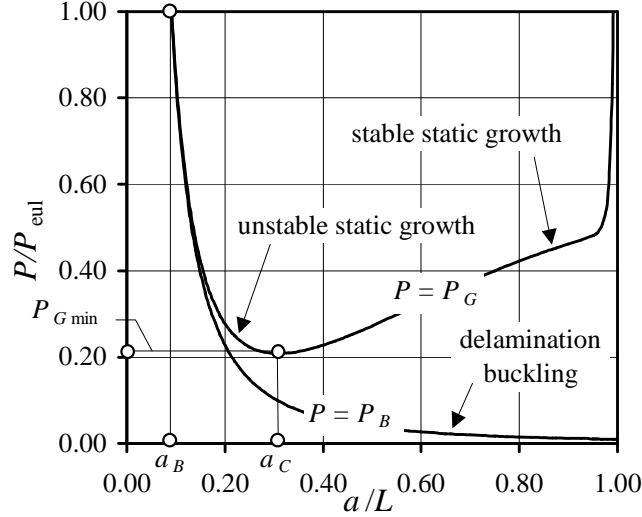


Fig. 2: Buckling load and static delamination growth load vs. delamination half-length

Two significant values of the delamination half-length have been highlighted in the figure: a_B , at which $P_B = P_{\text{eul}}$, and a_C , at which P_G reaches a local minimum, $P_{G\text{min}}$. If the length of the existing delamination is such that $a < a_B$, then local buckling phenomena and related delamination growth are not to be expected (although global instability can obviously occur); if, on the other hand, $a_B < a < a_C$, then delamination buckling and growth will be possible, the latter resulting in an unstable process; finally, if $a_C < a$, then delamination buckling and growth will be possible, though as a stable process.

For what follows it is useful to introduce an equivalent alternative formulation of the growth criterion. To this end, the energy release rate is normalized with respect to the mode-dependent toughness:

$$\hat{G} = \frac{G}{G_c(\psi)} \quad (5)$$

Consequently, under static loading, the condition for delamination growth becomes $\hat{G} = 1$, while no growth is instead predicted for $\hat{G} < 1$. With reference to Fig. 2, the static growth condition is fulfilled by points belonging to the 'growth curve', $P = P_G$. On the other hand, points located

below or on the ‘buckling curve’, $P = P_B$, furnish $\hat{G} = 0$. Lastly, for all points in the region between the above two curves, $0 < \hat{G} < 1$, no static growth is expected. However, delamination growth under cyclic loads is possible, as explained in the next paragraph. Finally, we should also note that \hat{G} turns out to be greater than 1 for all points located above the growth curve. This means that these points are not reachable via a quasi-static load history. Therefore, they have no meaning within the present model, which does not account for any dynamic effects.

FATIGUE DELAMINATION GROWTH

Moving on to examine the case of fatigue delamination growth, let us consider a laminated plate affected by a delamination whose initial half-length is a_0 . We assume that the applied compressive load varies cyclically between P_{\min} and P_{\max} , so that the energy release rate will vary between G_{\min} and G_{\max} . In these cases, experimental studies show that delamination growth can occur because of the progressive accumulation of damage at the delamination front as the delaminated plate undergoes repeated buckling and unloading.

According to [17], a fatigue growth law can be postulated,

$$\frac{da}{dN} = c(\psi) \frac{(\Delta \hat{G})^{m(\psi)}}{1 - \hat{G}_{\max}} \quad (6)$$

where N is the number of load cycles performed, and

$$\Delta \hat{G} = \frac{G_{\max} - G_{\min}}{G_c(\psi)} \quad (7)$$

is the range of the normalized energy release rate. In turn, $c(\psi)$ and $m(\psi)$ are two mode-dependent parameters to be determined by experiment. In particular, the multiplicative factor is

$$c(\psi) = c_I [1 + (\kappa - 1) \sin^2(\psi)] \quad (8)$$

where $\kappa = c_{II} / c_I$; c_I and c_{II} are the values measured in pure mode I and II tests, respectively.

Analogously, mode dependence is introduced for the exponent, by setting

$$m(\psi) = m_I [1 + (\mu - 1) \sin^2(\psi)] \quad (9)$$

where $\mu = m_{II} / m_I$; m_I and m_{II} are the values measured in pure mode I and II tests, respectively. The numerical values used for all subsequent figures are: $c_I = 50$ mm/cycle and $\kappa = 10$; $m_I = 10$ and $\mu = 0.50$.

In what follows we will assume that cycles are performed with $G_{\min} = 0$, so that $\Delta\hat{G} = \hat{G}_{\max}$, and the fatigue growth rate (6) becomes:

$$\frac{da}{dN} = c(\psi) \frac{(\hat{G}_{\max})^{m(\psi)}}{1 - \hat{G}_{\max}} \quad (10)$$

This assumption, however, does not necessarily imply $P_{\min} = 0$, but just that $P_{\min} \leq P_B$, since $G = 0$ in the pre-buckling phase.

The fatigue growth rate, da/dN , is a positive increasing function of \hat{G}_{\max} . Moreover, because of the denominator of equation (10), as \hat{G}_{\max} approaches unity, the growth rate goes to infinity, so that instant (static) growth is predicted. Also, da/dN is an increasing function of ψ (Fig. 3). Therefore, since the mode-mixity angle increases as the delamination grows longer [12], the growth rate is expected to become higher and higher as the process of fatigue growth itself develops. Fig. 4 represents da/dN as a function of the delamination half-length, a , at constant maximum load. The dashed curve is for $P_{\max} = P_{G\min}$: for this and all higher load values, da/dN features a vertical asymptote. Instead, for $P_{\max} < P_{G\min}$, the curves present a local maximum.

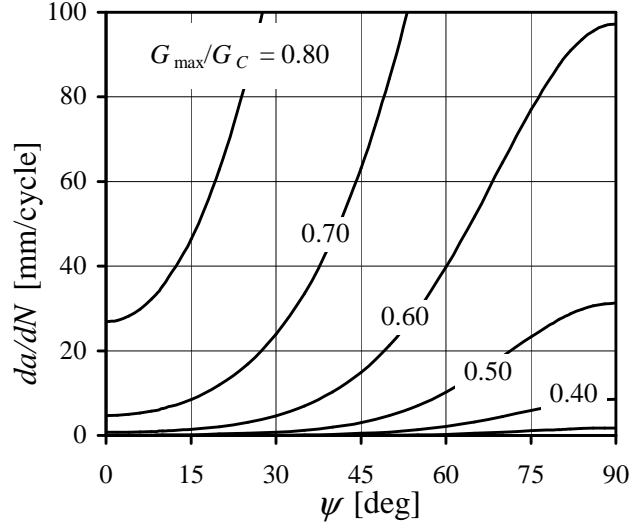


Fig. 3: Fatigue growth rate vs. mode-mixity angle

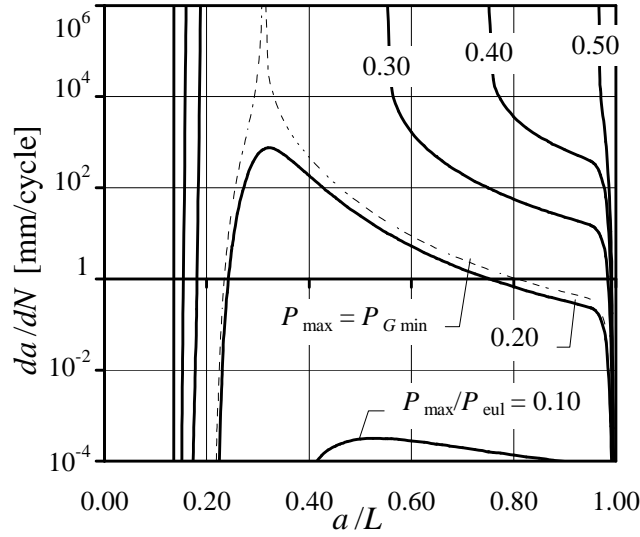


Fig. 4: Fatigue growth rate vs. delamination half-length

The number of cycles needed for the delamination to grow from its initial length, $2a_0$, to a current length, $2a$, is given by:

$$\Delta N(a_0, a) = \int_{a_0}^a \frac{dN}{d\bar{a}} d\bar{a} = \int_{a_0}^a \frac{1}{c(\psi)} \frac{1 - \hat{G}_{\max}}{(\hat{G}_{\max})^{m(\psi)}} d\bar{a}. \quad (11)$$

Because of the analytical complexity of equation (11), the integration must be carried out numerically. In the following, two cases are considered separately.

When the maximum load, P_{\max} , is less than the minimum load at which static growth can occur, $P_{G\min} = P_G(a_c)$, then the straight line, $P = P_{\max}$, intersects the buckling curve, $P = P_B$, at one

point where the delamination half-length, a_F , is such that $P_B(a_F) = P_{\max}$ (Fig. 5). If the initial delamination length is such that $a_0 \leq a_F$, then no fatigue growth is expected, since no local buckling will take place; instead, if $a_0 > a_F$, then fatigue growth is predicted. Moreover, fatigue growth will be ‘undefined’, since in theory it can continue until the plate is completely delaminated.

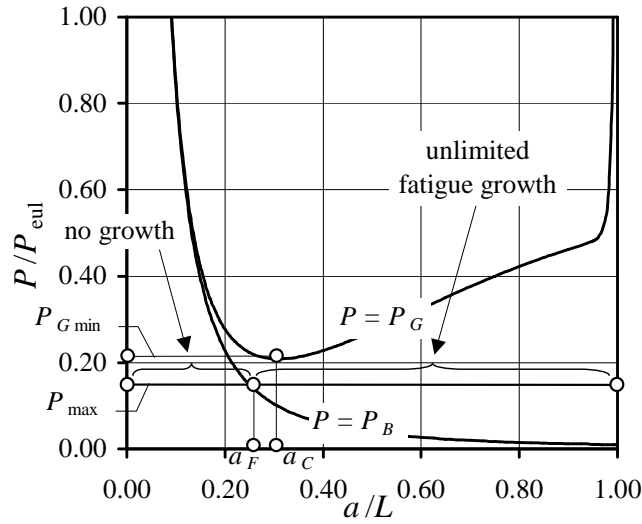


Fig. 5: Fatigue delamination growth ($P_{\max} \leq P_{G\min}$)

Instead, when the maximum load, P_{\max} , is greater than the minimum static growth load, $P_{G\min}$, then the straight line, $P = P_{\max}$, intersects the buckling curve, $P = P_B$, at a_F . It also intersects the growth curve, $P = P_G$, at two points where the delamination half-length is, respectively, a_{G1} and a_{G2} (Fig. 6). As in the previous case, if the initial delamination length is such that $a_0 \leq a_F$, then no fatigue growth is expected since no buckling will occur. Likewise, if $a_0 > a_{G2}$, then ‘undefined’ fatigue growth will take place. A different behaviour emerges in the range of $a_F < a_0 < a_{G1}$: here, fatigue growth is possible, but after a finite number of cycles have completed, at $a = a_{G1}$, the conditions for static growth are fulfilled and the process can possibly continue in the form of static growth until $a = a_{G2}$.

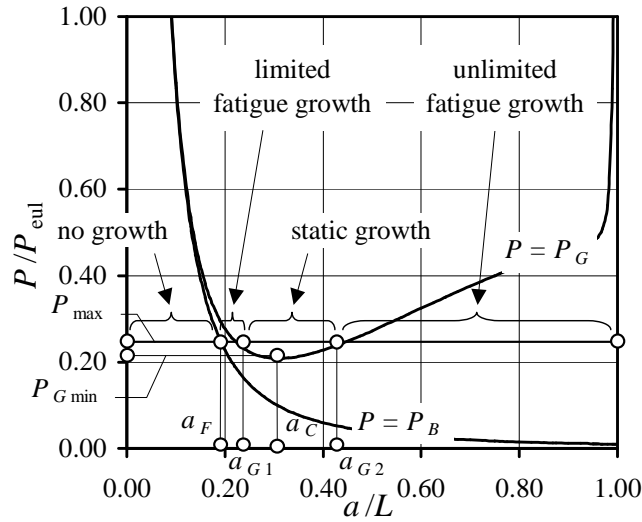


Fig. 6: Fatigue delamination growth ($P_{\max} > P_{G\min}$)

The following three figures show the delamination half-length as a function of the number of load cycles. A dashed line marks the value, a_F , for which no fatigue growth occurs. Depending upon the maximum load level, the qualitative trend of the fatigue growth process changes considerably. In Fig. 7, the load level is quite low ($P_{\max}/P_{eul} = 0.10$), and the delamination does not increase appreciably in length until more than 10^4 cycles have been performed. In Fig. 8, the maximum load ($P_{\max}/P_{eul} = 0.20$) is very close to the minimum static growth load ($P_{G\min}/P_{eul} = 0.2084$): here, rapid fatigue growth takes place, leading to complete delamination in a number of load cycles of less than 10^2 . Finally, in Fig. 9, the maximum load is $P_{\max} > P_{G\min}$. Here, for $a_0 > a_{G2}$, very rapid fatigue growth is expected, leading to complete delamination in less than 10 cycles. The curve for $a_0 = 0.20$ predicts peculiar behaviour, by which the delamination begins to grow very slowly, then, at $a = a_{G2}$, it suddenly makes a ‘jump’ leading to complete delamination. Such behaviour clearly represents a very insidious and dangerous failure mode.

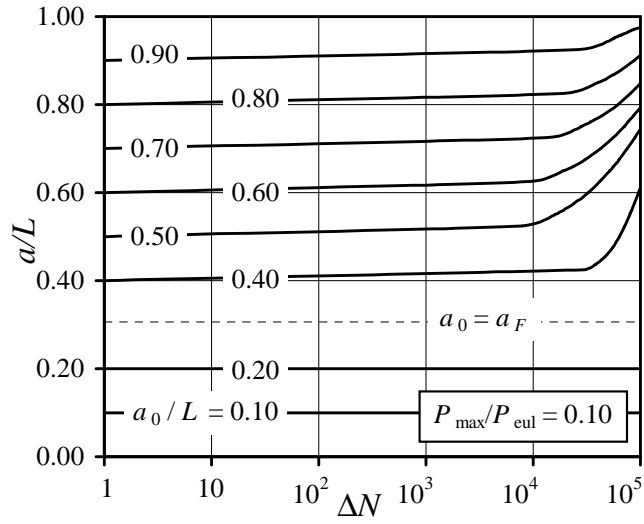


Fig. 7: Delamination half-length vs. number of load cycles at $P_{\max} = 0.10 P_{\text{eul}}$

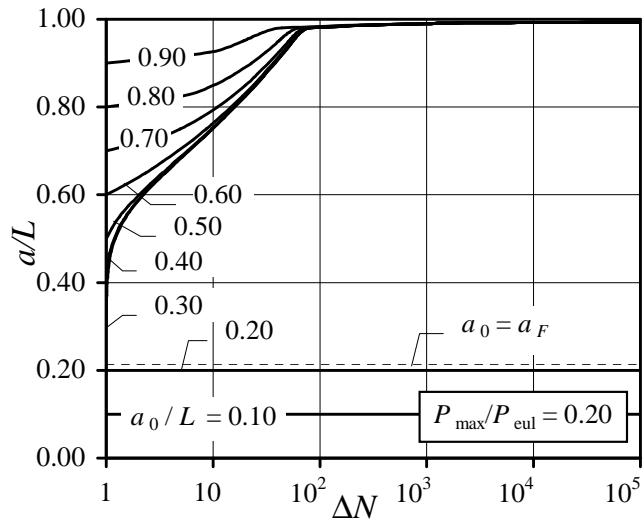


Fig. 8: Delamination half-length vs. number of load cycles at $P_{\max} = 0.20 P_{\text{eul}}$

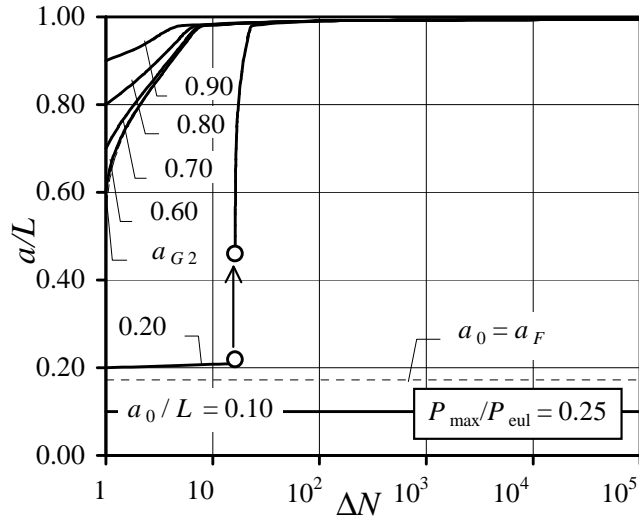


Fig. 9: Delamination half-length vs. number of load cycles at $P_{\max} = 0.25 P_{\text{eul}}$

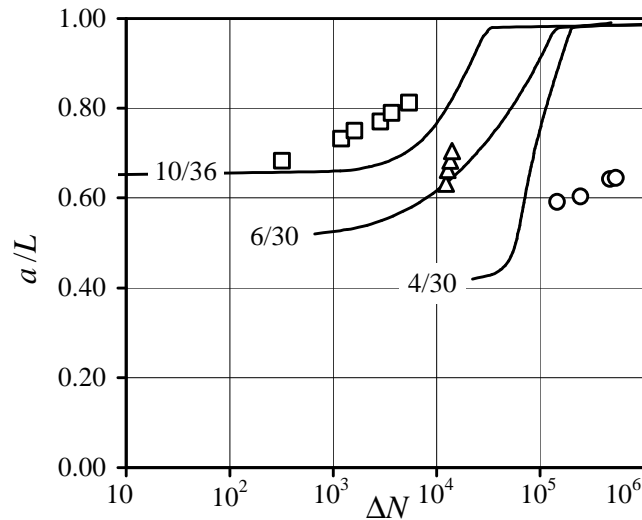


Fig. 10: Delamination half-length vs. number of load cycles: theoretical predictions and experimental results

As a last example, Fig. 10 shows a comparison between the theoretical predictions of the present model (continuous lines) and some experimental results (single points) reported in [17]. The experiments concerned the three graphite-epoxy specimens described in Table 1: specimen 10/36 was a 36-ply laminate having a delamination between the tenth and eleventh plies; specimens 6/30 and 4/30 were 30-ply laminates containing delaminations, respectively, between the sixth and seventh and between the fourth and fifth plies.

Table 1: Specimen data (from [17]).

Specimen	Thickness H [mm]	Delamination half-length		Maximum strain/load		
		a_0 [mm]	a_0 / L	ϵ_{\max}	$P_{\max} = A\epsilon_{\max}$ [N/mm]	P_{\max}/P_{eul}
10/36 (\square)	2.87	33.02	0.650	1.003×10^{-3}	456.2	0.350
6/30 (Δ)	2.75	26.15	0.515	1.325×10^{-3}	552.4	0.550
4/30 (\circ)	2.75	21.25	0.418	1.575×10^{-3}	685.3	0.600

Moreover, the following values drawn from the cited paper were used: $L = 50.8$ mm, $E_X^* = 151.6$ GPa, $G_{IC} = 190$ J/m², $\gamma = G_{IC} / G_{IIC} = 0.30$; finally, the fatigue growth law parameters were assumed to be $c_I = 0.0435$ mm/cycle, $\kappa = 10.1$, $m_I = 10.385$ and $\mu = 0.501$.

Only the 6/30 specimen yields a good fit between theory and experiments; conversely, theoretical predictions for the 10/36 and 4/30 specimens appear, respectively, to overestimate and underestimate the actual fatigue lifetime. Further studies are needed to determine the reasons for such discrepancies.

CONCLUSION

Knowing the explicit expressions for the normal and tangential interlaminar stresses and their peak values at the delamination front produced by compression cycles able to trigger local instability mechanisms allows for direct calculations of the intensity oscillations of the crack driving forces and. Once the fatigue delamination growth criterion has been chosen, this enables following the history of the spread of the delaminated region. Growth by fatigue is in fact a complex phenomenon: one needs only consider how the so-called mixity angle gradually changes during the growth of the delamination and, with it, the relative contributions of mode I and II involved in the extension process. In this perspective, the possibility of direct calculations offered by the very simple mechanical model could prove to be a precious aid in explaining the reasons why small changes in the governing parameters (such as the initial delamination length, the intensity of the maximum load, significant mechanical parameters of the composite laminate, etc.) can lead to

completely different pathways of delamination growth. Further work is planned to verify this hypothesis by an accurate comparison with the experimental data available in the literature, as well as by carrying out expressly designed specific experimental tests.

REFERENCES

1. Garg A C. Delamination – A damage mode in composite structures. *Eng Fract Mech* 1988; 29: 557-584.
2. Abrate S. Impact on laminated composite materials. *Appl Mech Reviews* 1991; 44: 155-190.
3. Bolotin V V. Delaminations in composite structures: its origin, buckling, growth and stability, *Compos Part B-Eng* 1996; 27: 129-145.
4. Kachanov L M. Delamination buckling of composite materials. Dordrecht-Boston-London: Kluwer Academic Publishers, 1988.
5. Storåkers B. Nonlinear aspects of delamination in structural members. *Proceedings of the 17th International Congress of Theoretical and Applied Mechanics (Grenoble, France, 1988)*, Amsterdam: North-Holland, Elsevier Science Publishers, 1989. p. 315-336.
6. Chai H, Babcock C D, Knauss W G. One dimensional modelling of failure in laminated plates by delamination buckling, *Int J Solids Struct* 1981; 17: 1069-1083.
7. Yin W-L, Wang J T-S. The energy-release rate in the growth of a one-dimensional delamination, *J Appl Mech-T ASME* 1984; 51: 939-941.
8. Whitcomb J D. Finite element analysis of instability related delamination growth, *J Compos Mater* 1981; 15: 403-426.
9. Hutchinson J W, Suo Z. Mixed mode cracking in layered materials, *Adv Appl Mech* 1992; 29: 63-191.
10. Valvo P S. Fenomeni di instabilità e di crescita della delaminazione nei laminati compositi. Ph.D. Thesis, University of Florence, Department of Civil Engineering, 2000 (in Italian).

11. Bennati S, Valvo P S. An elastic-interface model for delamination buckling in laminated plates, *Key Eng Mat* 2002; 221-222: 293-306.
12. Bennati S, Valvo P S. A mechanical model for mixed-mode buckling-driven delamination growth. *Atti del XV Congresso Nazionale, Taormina, Italy: 2001* (full text on CD Rom).
13. Vizzini A J, Lagace P A. The buckling of a delaminated sublaminates on an elastic foundation, *J Compos Mater* 1987; 21: 1106-1117.
14. Bruno D, Grimaldi A. Delamination failure of layered composite plates loaded in compression, *Int J Solids Struct* 1990; 26: 313-330.
15. Corigliano A. Formulation, identification and use of interface models in the numerical analysis of composite delamination, *Int J Solids Struct* 1993; 30: 2779-2811.
16. Point N, Sacco E. A delamination model for laminated composites, *Int J Solids Struct* 1996; 33: 483-509.
17. Kardomateas G A, Pelegri A A, Malik B. Growth of internal delaminations under cyclic compression in composite plates, *J Mech Phys Solids* 1995; 43: 847-868.